

Original**Expression of Keratin 75 (K6hf) in Oral Squamous Cell Carcinoma**

Shizunari OBARA, Gou YAMAMOTO, Shigeo HAYASHI, Jun-Ichi TANAKA,
Tomohide ISOBE, Chie HOKAZONO, Rika YASUHARA, Tarou IRIE
and Tetsuhiko TACHIKAWA

*Department of Oral Pathology and Diagnosis, Showa University School of Dentistry
1–5–8 Hatanodai, Shinagawa-ku, Tokyo, 142–8555 Japan
(Chief: Prof. Tetsuhiko Tachikawa)*

Abstract: Cytokeratin is commonly used diagnostic markers of oral squamous cell carcinoma (OSCC). Especially, Keratin17 (K17) is reported to be up-regulated in OSCC. Recently, identification and quantification of proteins from tissue section become possible by using laser microdissection and LC/MS/MS method. In this study, we performed nano-flow liquid chromatography, mass spectrometry and protein identification by tandem mass spectrometry (LC/MS/MS) analysis on pooled protein extracts from OSCC tissue section and compared the results with those from normal epithelium. As a result, Keratin 6hf is considered as a candidate marker of OSCC. From more validation, the expression of K6hf may be associated with malignancy of oral epithelial lesion. In previous study, K6hf is known to be specifically expressed in a hair follicle and specifically cross a partner with K17. But, there are no report about correlation between K6hf and carcinoma. In conclusion, K6hf expression may play an important role in the carcinogenesis progression of OSCC. However, further studies on the molecular function of K6hf are encouraged to clear the precise mechanism of K6hf in OSCC.

Key words: keratin 6hf, oral squamous cell carcinoma, LC/MS/MS, laser microdissection.

Oral squamous cell carcinoma (OSCC) is one of the most common malignancies in the head and neck region, afflicting about 300,000 patients worldwide each year.^{1,2)} For many years, the 5-year survival rate of OSCC patients has remained relatively low, only approximately 50–60%^{3,4)} and the rate is even lower in patients diagnosed at later stages. Although early diagnosis and efficient treatment are the keys to the prognosis of OSCC, up to date, specific biomarkers for early diagnosis and prognostic monitoring of OSCC are lacking.

Cytokeratin is over-expressed in tumor tissue compared to normal oral mucosa.^{5~7)} Furthermore Keratin 13 (K13) is decreased in OSCC.⁸⁾ Therefore, these cytokeratin alterations may be used as diagnostic marker of OSCC.

The type II keratin 75 (keratin 6hf; K6hf) has been described as being specifically expressed in the

companion layer of the hair follicle⁹⁾ in human skin. This distinct compartment consists of a single layer of flattened cells located at the interface between the outer root sheath, a stratified epithelium contiguous with the epidermis, and the inner root sheath, a three-layered compartment located between the companion layer and hair shaft.^{9~11)} However, correlation of OSCC and K6hf remains unclear.

In recent years, proteomics has emerged as a powerful technology to identify differential protein expressions associated with cancer development and progression. In particular, laser microdissection and LC/MS/MS method using tissue sections accompanied by both definitive diagnoses and known clinical outcomes provide a great opportunity for biomarker discovery.^{12~15)}

In this study, we use this method and try to discover biomarker of OSCC. As a result, K6hf is identified

as a candidate marker. This report is the first paper describing about K6hf expression in carcinoma, furthermore in tissue except a hair follicle.

Materials and Methods

Sample preparation

Primary tumor samples were obtained, with informed consent, from patients undergoing surgery for OSCC as a primary treatment without previous radiation or chemotherapy. All samples were immediately placed on ice and a tumor fragment was taken the primary tumor. The extracted tissues were embedded in OCT compound and frozen in isopentane cooled in liquid nitrogen. The tissues were then made into a frozen block, which was sliced with at cryomicrotome at 4 μm thickness for immunohistochemistry. For the microdissection, the frozen sections sliced at 7 μm (real-time PCR) and 10 μm (LC/MS/MS) were placed on film slide glass, and stored at -40°C .

Laser microdissection

For real-time PCR, the frozen sections were placed at room temperature for 1–2 min and fixed in 100% methanol for 3 min. After washing with 50% ethanol, the sections were stained with crystal violet (Ambion, USA). Finally, sections were washed with 100% ethanol, and they were air-dried. The sections were microdissected with a PALM[®] Micro Beam (Carl Zeiss Microimaging, Germany). The target areas were normal epithelium, epithelial dysplasia and OSCC from the cancer patients. From the type of well differentiated regions that form a cancer peal, we removed the keratinized area in advance. There were estimated to be approximately 500–2,000 microdissected cells per sample.

For LC/MS/MS, the frozen sections were stained with mayer's hematoxylin (Sakura finetek, Japan) and washed with distilled water. The target areas were normal epithelium and OSCC. Microdissected cells per samples were approximately 30,000 cells.

Analysis by Nano-UPLC-MS^E Tandem Mass Spectrometry

Collected tissue from sections was subjected to in-solution trypsin digestion as described previously.¹⁶⁾ Digested samples were desalted and concentrated using Sep-Pak C₁₈ column cartridges (Waters, USA) according to the manufacturer's instructions. Samples were analyzed by nano-UPLC-MS^E using a 75- μm -inner diameter \times 25-cm C₁₈ nanoAcquity[™] UPLC[™] column (1.7- μm particle size; Waters) and a 90-min gradient: 2–45% solvent B (solvent A: 99.9% H₂O, 0.1% formic acid; solvent B: 99.9% acetonitrile, 0.1% formic acid) on a Waters nanoAcquity UPLC system (final flow rate, 250 nl/min; 7000 p.s.i.) coupled to a Waters QTOFpremier[™] tandem mass spectrometer. Data were acquired in high definition MS^E mode (low collision energy, 4 eV; high collision energy ramping from 15 to 40 eV, switching every 1.5 s) and processed with ProteinLynx Global Server (PLGS; version 2.2.5; Waters) to reconstruct MS/MS spectra by combining all masses with identical retention times. Each sample was analyzed in triplicate runs. The mass accuracy of the raw data was corrected using Glu-fibrinopeptide (200 fmol/ μl , 700 nl/min flow rate, 785.8426 Da [$\text{M} + 2\text{H}$]²⁺) that was infused into the mass spectrometer as a lock mass during sample analysis. Low and high collision energy MS data were calibrated at intervals of 30 s. The raw data sets were processed including deisotoping and deconvolution, and peak lists were generated on the basis of assigning precursor ions and fragments based on similar retention times.^{17, 18)} A Swiss-Prot database was used for database searches of each triplicate run with the following parameters: peptide tolerance, 15 ppm; fragment tolerance, 0.015 Da; trypsin missed cleavages, 1; and variable modifications, carbamidomethylation and Met oxidation. Alternatively MS/MS spectra (peak lists) were also searched against the Swiss-Prot database using Mascot version 2.2 (Matrix Science, UK) and the following parameters: peptide tolerance, 0.2 Da; ¹³C = 2; fragment tolerance, 0.1 Da; missed cleavages, 3; and

instrument type, ESI-Q-TOF. The interpretation and presentation of MS/MS data were performed according to published guidelines.¹⁹⁾ In addition, individual MS/MS spectra for peptides with a Mascot Mowse (molecular weight search) score lower than 40 (expect value <0.015) were inspected manually and included in the statistics only if a series of at least four continuous y or b ions were observed. Protein identification was also based on the assignment of at least two peptides. False positive rates for the data sets generated in this study were evaluated using Mascot and a randomized database based on Swiss-Prot (decoy function).

Quantitative analysis

The analysis of quantitative changes in protein abundance, which is based on measuring peptide ion peak intensities observed in low collision energy mode in a triplicate set, was carried out using Waters Expression Analysis Software (WEPS™), which is part of PLGS 2.2.5 (Expression version 2). For normalization, each sample was spiked with 125 fmol of tryptic digest of α -enolase as an internal standard. Included were all protein hits that were identified with a confidence of >95%. Identical peptides from each triplicate set per sample were clustered based on mass precision (<15 ppm, typically ~5 ppm) and a retention time tolerance of <0.25 min using the clustering software included in PLGS 2.2.5. Protein scores were increased when the same peptide assignments were made in more than one replicate run. To avoid potential errors due to redundancies in assignments, searches were performed using the non-redundant Swiss-Prot database (as described above). Furthermore if two or more distinct proteins shared an identical peptide but were found to be regulated differently, then the quantitation algorithm did not include the peptide in question. To allow for this, peptide probabilities are always softened slightly by the PLGS software prior to quantitation. Because of this, the contributions from peptides with even 100% probability of presence were suppressed to avoid potential errors in quantitation.

Normalization of the data sets was performed based on the spiked standard, but very similar results were obtained using the PLGS “autonormalization” function (not shown).

Real-time PCR

For real-time RT-PCR analysis, total RNA was extracted from laser-microdissected cells using the RNeasy Micro Kit (QIAGEN, Germany). cDNA from total RNA were synthesized using the High Capacity cDNA Archive according to the manufacture’s instruction. The relative quantification (RQ) of mRNA was performed with the ABI 7500 Fast Real-Time PCR System (Applied Biosystems, USA). The High Capacity RNA-to-cDNA Master Mix reagents (Applied Biosystems) were used for PCR amplification. Reverse transcription was done using 16 μ l of total RNA from patient samples. The resulting cDNA was stored at -20°C until further use. From this cDNA solution, 2 μ l was removed to be subsequently used for the real-time RT-PCR reaction, 10 μ l the TaqMan® Gene Expression Master Mix reagents (Applied Biosystems) containing 1 μ l TaqMan® gene expression assay (Applied Biosystems) was used at 20 μ l/tube.

The RT-PCR assay was performed using the Applied Biosystems 7500 Fast Real-Time PCR System (Applied Biosystems) with the following profile; 1 cycle at 50°C for 2 min, 1 cycle at 95°C for 10 min, and 50 cycles each at 95°C for 15 s and 50°C for 1 min. With the threshold cycle (Ct) values detected by this system, relative quantification of K6hf (Assay ID: Hs00190778) mRNA level compared with internal control gene GAPDH (Assay ID: Hs99999905) was calculated according to the ΔCt method.

Immunohistochemical study

Immunohistochemical analysis using the DAKO EnVision system (DAKO, USA) was performed. The frozen sections were fixed for 30 min in 4% paraformaldehyde, and washed with phosphate-buffered solution (PBS, pH7.4) 3 times for 3 min

each. Blocking reagent (DAKO) was then applied at room temperature for 10 min to prevent nonspecific binding of antibodies, and the sections were washed PBS 3 times for 3 min each. In this study, anti-K6hf mouse monoclonal (Lifespan Bioscience, USA) was used. The antibody was diluted 200× and dropped onto the sections for 30 min at room temperature. The sections were incubated with polymer reagent (DAKO EnVision) for 30 min. After washing with PBS, the sections were incubated with 3,3'-diaminobenzidine tetrahydrochloride (DAKO) for 1–2 min. Finally, sections were washed with distilled water, counterstained with hematoxylin for 1 min, washed with tap water and ethanol, and covered with coverslips.

Results

Protein identification by LC/MS/MS

We used 2 cases of OSCC for LC/MS/MS analysis

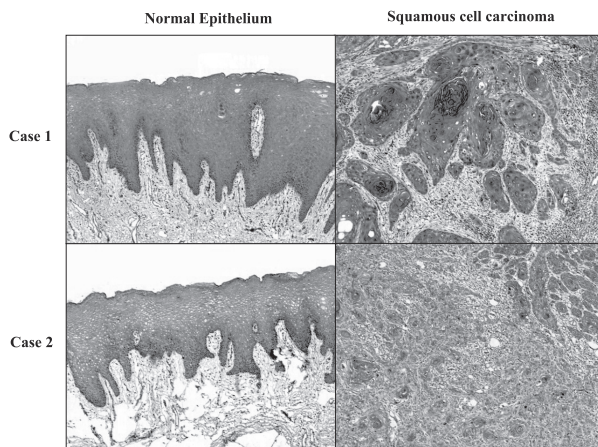


Fig. 1 H.E.staining of each cases for LC/MS/MS analysis (magnification: ×50).

(Fig. 1). From each case, normal epithelium and OSCC were collected. The identification results of protein for triplicate injections were merged and proteins detected twice or more were used for in the discussion of this study. In comparison of two normal epitheliums, many kinds of proteins were common. However, in other combinations, those were varied (Fig. 2). After quantitative analysis, we confirmed about known markers, K 13, 17 and CD98^{8, 20, 21}) and validated whether this experiment reflected each lesion. In addition, we identified K6hf as a candidate marker of OSCC (Table 1).

Gene expression of K6hf in tissue section

To confirm the validity of the LC/MS/MS results, real-time semi-quantitative RT-PCR was performed with a set of human-specific primers and template cDNA generated by reverse-transcription. Similar to the LC/MS/MS results, the level of K6hf expression

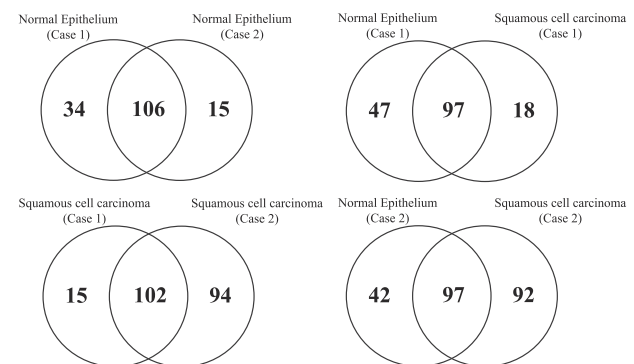


Fig. 2 Venn diagram of detected proteins. Only comparison between normal epithelium indicated a similar protein expression profile.

Table 1 Protein quantification of already known markers and candidate marker.

Protein name	Normal epithelium (case1)		Normal epithelium (case2)		OSCC (case1)		OSCC (case2)	
	Amount (fmol)	Amount (ngrams)	Amount (fmol)	Amount (ngrams)	Amount (fmol)	Amount (ngrams)	Amount (fmol)	Amount (ngrams)
K17	6	0.3	2.3	0.1	65.7	3.2	96.8	4.7
K13	561.9	27.9	604.5	30	5.6	0.3	4.2	0.2
CD98 (SLC3A2)	N.D		N.D		2.4	0.2	2.1	0.1
K6hf	0.7	0.07	N.D		2.2	0.2	4.9	0.4

The LC/MS/MS system (LC/MSE) is the ability to generate absolute quantification values for each identified protein that contains more than two peptides and it allows us to sort unique proteins for each sample by their abundance. We selected K6hf as a candidate marker shown in the table above. (N.D; not detectable).

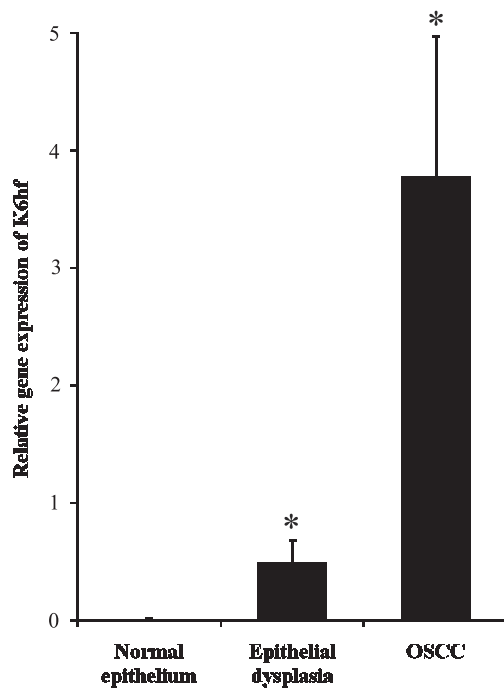


Fig. 3 Gene expression of K6hf in frozen tissue sections. As a result of real-time PCR, in the gene expression of K6hf, there was a large difference between normal epithelium and squamous cell carcinoma. (Bar; 1SD, *, $p < 0.05$)

in the OSCC was significantly higher than in the normal epithelium (Fig. 3). In this analysis, epithelial dysplasia was added to our study. As a result, K6hf gene expression in that lesion was intermediate degree of normal epithelium and epithelial dysplasia. These data suggested that the gene expression of K6hf was increased with a process of carcinogenesis. Moreover, K6hf could be a characterized marker of the OSCC.

Immunohistochemical analysis of K6hf localization

To confirm the expression of the K6hf protein within the carcinogenesis, we performed immunostaining of the normal epithelium, epithelial dysplasia and OSCC.

As shown in Fig. 4, K6hf localized specifically in tumor cells of OSCC. In mild epithelial dysplasia, few of epithelial cells were stained positively (Fig. 5). In sever epithelial dysplasia, almost all of cells were stained as compared to mild epithelial dysplasia (Fig. 5). These data suggested that K6hf was characteristically

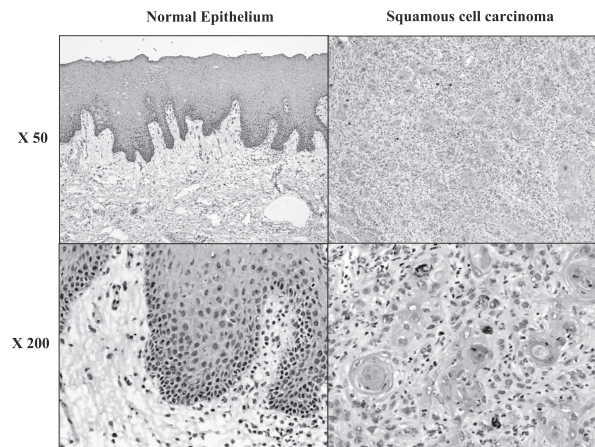


Fig. 4 Immunohistochemical staining of K6hf in normal epithelium and OSCC. Normal epithelium stained negative. Squamous cell carcinoma indicated positive reaction.

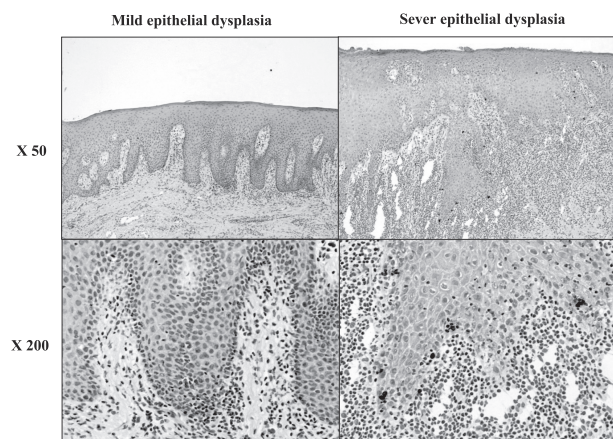


Fig. 5 Immunohistochemical staining of K6hf in mild and sever epithelial dysplasia. In mild epithelial dysplasia, only a few cells were stained positive. On the other hand, in sever dysplasia, a positive cell was observed similar to squamous cell carcinoma.

expressed in malignant epithelial cells.

Discussion

K6hf is one of the isoforms of the keratin 6 (K6) family located within the type II cytokeratin gene cluster on chromosome 12 of humans and chromosome 15 of mice.²²⁾ About K6hf, the expression in tissue is unknown except a hair follicle. In tumor, the only one report describes about cylindrome.²³⁾

Since keratin IFs (KIFs) assemble from heterodimers made up of one type I and one type II keratin,^{24, 25)}

keratins are generally considered to be coexpressed with specific partners of the opposite type. K6, a type II keratin, is thought to have two type I partners, K16 and K17. Especially, K17 was reported as a specific partner of K6hf.²⁶⁾

K6 isoforms are specifically induced in response to hyperproliferative stimuli, such as wounding. For example, K6A is induced in all layers of the epidermis under hyperproliferative conditions, whereas the induction of K6b is restricted to the more differentiated layers of the epidermis.²⁷⁾ The *in vivo* functions of K6 genes have been evaluated in genetically engineered mouse models for K6a (K6a^{tm1Der}) and K6a/K6b (K6a/K6b^{tm1Cou}, K6a/ K6b^{tm1Der}).^{27~29)} Interestingly, the absence of K6a or K6a/K6b did not prevent normal development and function of epithelial tissues and ectodermal appendages. However, loss of these proteins altered the response of these tissues to injury and mechanical stress. For instance, delayed re-epithelialization of the skin was observed in Krt6a^{tm1Der} mice following wounding,²⁷⁾ and hyperplastic changes secondary to mechanical stress associated with food intake were reported in the oral cavities of K6a/K6b^{tm1Cou} and K6a/K6b^{tm1Der} mice.^{28,29)} In the area of hyperplastic change, a expression of K17 was strongly observed. Moreover, K6a/K6b-null explants exhibited a statistically significant 1.8-fold enhancement of epithelial outgrowth as compared with wild-type and hemizygous explants.³⁰⁾ In contrast to K6a and K6b, K6hf expression is not induced in the epidermis in response to mechanical stress or wounding.²⁸⁾

But, mutation of K6hf caused pachyonychia congenital same as K6a and b.³¹⁾ From those studies, it was suggested that K6a/b and K6hf had similar characterization but a different function might be present. In addition, K17 played important role in cell growth and migration without K6. K17 was considered as diagnostic marker of OSCC and was reported to regulate protein synthesis and epithelial cell growth.³²⁾ Our result indicates that K6hf localized in epithelial cells of malignant change. In OSCC, because a partner

of K17 changes into K6hf from K6, a function of K17 might be affected. As a result, K6hf was considered as a diagnostic marker of OSCC.

Acknowledgments This work was supported in part by an innovative research project of oral cancer based on molecular basis: from elucidation of the causal mechanisms to the improvement of Quality of Life through oral rehabilitation and Grants for the promotion of the advancement of education and research in graduate schools and High-Tech Research Center Project for Private Universities from the Ministry of Education, Culture, Sports, Science and Technology, Japan.

References

- 1) Petersen PE: The World Oral Health Report 2003: continuous improvement of oral health in the 21st century—the approach of WHO Global Oral Programme. *Community Dent Oral Epidemiol*, **31**: 3–23, 2003
- 2) Kademani D: Oral cancer. *Mayo Clin Proc*, **82**: 878–887, 2007
- 3) Neville BW, Day TA: Oral cancer and precancerous lesions. *CA Cancer J Clin*, **52**: 195–215, 2002
- 4) Parkin DM, Bray F, Ferlay J, Pisani P: Global cancer statistics, 2002. *CA Cancer J Clin*, **55**: 74–108, 2005
- 5) Moll R, Krepler R, Franke WW: Complex cytokeratin polypeptide patterns observed in certain human carcinomas. *Differentiation*, **23**: 256–269, 1983
- 6) Lane EB, Alexander CM: Use of keratin antibodies in tumor diagnosis. *Semin Cancer Biol*, **1**: 165–179, 1990
- 7) Chu PG, Weiss LM: Keratin expression in human tissues and neoplasms. *Histopathology*, **40**: 403–439, 2002
- 8) Bloor BK, Seddon SV, Morgan PR: Gene expression of differentiation-specific keratins in oral epithelial dysplasia and squamous cell carcinoma. *Oral Oncol*, **37**: 251–261, 2001.
- 9) Winter H, Langbein L, Praetzel S, Jacobs M, Rogers MA, Leigh IM, Tidman N, Schweizer J: A novel human type II cytokeratin, K6hf, specifically expressed in the companion layer of the hair follicle. *J Invest Dermatol*, **111**: 955–962, 1998
- 10) Rothnagel JA, Roop DR: Hair follicle companion layer: Reacquainting an old friend. *J Invest Dermatol*, **104**: S42–S43, 1995
- 11) Langbein L, Rogers MA, Praetzel S, Aoki N, Winter H, Schweizer J: A novel epithelial keratin, hK6irs1, is expressed differentially in all layers of the inner root sheath, including specialized Huxley cells (Flugelzellen) of the human hair follicle. *J Invest Dermatol*, **118**: 789–799,

- 2002
- 12) Prieto DA, Hood BL, Darfler MM, Guiel TG, Lucas DA, Conrads TP, Veenstra TD, Krizman DB: Liquid Tissue™: proteomic profiling of formalin-fixed tissues. *BioTechniques*, **38**: S32–S35, 2005
 - 13) Hood BL, Darfler MM, Guiel TG, Furusato B, Lucas DA, Ringeisen BR, Sesterhenn IA, Conrads TP, Veenstra TD, Krizman DB: Proteomic analysis of formalin-fixed prostate cancer tissue. *Mol Cell Proteomics*, **4**: 1741–1753, 2005
 - 14) Hood BL, Conrads TP, Veenstra TD: Unravelling the proteome of formalin-fixed paraffin-embedded tissue. *Brief Funct Genomic Proteomic*, **5**: 169–175, 2006
 - 15) Hood BL, Conrads TP, Veenstra TD: Mass spectrometric analysis of formalin-fixed paraffin-embedded tissue: Unlocking the proteome within. *Proteomics*, **6**: 4106–4114, 2006
 - 16) Kinter M, Sherman NE: *Protein Sequencing and Identification Using Tandem Mass Spectrometry*. New York, 2000, Wiley Interscience, pp 147–164
 - 17) Silva JC, Denny R, Dorschel C, Gorenstein MV, Li GZ, Richardson K, Wall D, Geromanos SJ: Simultaneous qualitative and quantitative analysis of the *Escherichia coli* proteome: a sweet tale. *Mol Cell Proteomics*, **5**: 589–607, 2006
 - 18) Silva JC, Gorenstein MV, Li GZ, Vissers JP, Geromanos SJ: Absolute quantification of proteins by LCMSE: a virtue of parallel MS acquisition. *Mol Cell Proteomics*, **5**: 144–156, 2006
 - 19) Taylor GK, Goodlett DR: Rules governing protein identification by mass spectrometry. *Rapid Commun Mass Spectrom*, **19**: 3420, 2005
 - 20) Kim DK, Ahn SG, Park JC, Kanai Y, Endou H, Yoon JH: Expression of L-type amino acid transporter 1 (LAT1) and 4F2 heavy chain (4F2hc) in oral squamous cell carcinoma and its precursor lesions. *Anticancer Res*, **24**: 1671–1675, 2004
 - 21) Wei KJ, Zhang L, Yang X, Zhong LP, Zhou XJ, Pan HY, Li J, Chen WT, Zhang ZY: Overexpression of cytokeratin 17 protein in oral squamous cell carcinoma in vitro and in vivo. *Oral Dis*, **15**: 111–117, 2009
 - 22) Schweizer J, Bowden PE, Coulombe PA, Langbein L, Lane EB, Magin TM, Maltais L, Omary MB, Parry DA, Rogers MA, Wright MW: New consensus nomenclature for mammalian keratins. *J Cell Biol*, **174**: 169–174, 2006
 - 23) Massoumi R, Podda M, Fässler R, Paus R: Cylindroma as tumor of hair follicle origin. *J Invest Dermatol*, **126**: 1182–1184, 2006
 - 24) Hatzfeld M, Weber K: The coiled coil of in vitro assembled keratin filaments is a heterodimer of type I and II keratins: use of site-specific mutagenesis and recombinant protein expression. *J Cell Biol*, **110**: 1199–1210, 1990
 - 25) Steinert PM: The two-chain coiled-coil molecule of native epidermal keratin intermediate filaments is a type I-type II heterodimer. *J Biol Chem*, **265**: 8766–8774, 1990
 - 26) Wang Z, Wong P, Langbein L, Schweizer J, Coulombe PA: Type II epithelial keratin 6hf (K6hf) is expressed in the companion layer, matrix, and medulla in anagen-stage hair follicles. *J Invest Dermatol*, **121**: 1276–1282, 2003
 - 27) Wojcik SM, Bundman DS, Roop DR: Delayed wound healing in keratin 6a knockout mice. *Mol Cell Biol*, **20**: 5248–5255, 2000
 - 28) Wojcik SM, Longley MA, Roop DR: Discovery of a novel murine keratin 6 (K6) isoform explains the absence of hair and nail defects in mice deficient for K6a and K6b. *J Cell Biol*, **154**: 619–630, 2001
 - 29) Wong P, Colucci-Guyon E, Takahashi K, Gu C, Babinet C, Coulombe PA: Introducing a null mutation in the mouse K6alpha and K6beta genes reveals their essential structural role in the oral mucosa. *J Cell Biol*, **150**: 921–928, 2000
 - 30) Wong P, Coulombe PA: Loss of keratin 6 (K6) proteins reveals a function for intermediate filaments during wound repair. *J Cell Biol*, **163**: 327–337, 2003
 - 31) Chen J, Jaeger K, Den Z, Koch PJ, Sundberg JP, Roop DR: Mice expressing a mutant Krt75 (K6hf) allele develop hair and nail defects resembling pachyonychia congenita. *J Invest Dermatol*, **128**: 270–279, 2008
 - 32) Kim S, Wong P, Coulombe PA: A keratin cytoskeletal protein regulates protein synthesis and epithelial cell growth. *Nature*, **441**: 362–365, 2006